

Article

# Simulation Process for Allyl Alcohol Production via Deoxydehydration of Glycerol

Ghadir Assaad, Karen Silva Vargas, Benjamin Katryniok \* and Marcia Araque

Université de Lille, CNRS, Centrale Lille, Université d'Artois, UMR 8181—Unité de Catalyse et Chimie du Solide (UCCS), 59000 Lille, France; ghadir.assaad@univ-lille.fr (G.A.); karen.silva-vargas@orano.group (K.S.V.); marcia-carolina.araque-marin@centralelille.fr (M.A.)

\* Correspondence: benjamin.katryniok@centralelille.fr

**Abstract:** A process for the deoxydehydration (DODH) of glycerol to allyl alcohol in 2-hexanol as solvent was modelled with Aspen Plus. Experimental results for the DODH reaction, the liquid vapour equilibria and the catalytic hydrogenation were employed for the development of the model. The whole process consists of four subsystems: allyl alcohol production (S1), solvent recovery (S2), allyl alcohol purification (S3) and solvent regeneration (S4). Based on the results of the process model, allyl alcohol with 96% yield and a purity of 99.99% with product loss of only 0.2% was obtained. The optimisation of the energy consumption through an integrated heat exchange network resulted in a net primary energy input of 863.5 kW, which corresponded to a carbon footprint of 1.89 kgCO<sub>2</sub>/kgAllylOH.

**Keywords:** glycerol; allyl alcohol; process simulation; ASPEN; deoxydehydration



**Citation:** Assaad, G.; Silva Vargas, K.; Katryniok, B.; Araque, M. Simulation Process for Allyl Alcohol Production via Deoxydehydration of Glycerol. *ChemEngineering* **2024**, *8*, 10. <https://doi.org/10.3390/chemengineering8010010>

Academic Editors: Roberto Rosa, Anna Maria Ferrari, Consuelo Mugoni and Grazia Maria Cappucci

Received: 12 September 2023

Revised: 16 October 2023

Accepted: 1 December 2023

Published: 3 January 2024



**Copyright:** © 2024 by the authors. Licensee MDPI, Basel, Switzerland. This article is an open access article distributed under the terms and conditions of the Creative Commons Attribution (CC BY) license (<https://creativecommons.org/licenses/by/4.0/>).

## 1. Introduction

Allyl alcohol holds great potential as a versatile molecule with a wide array of applications. Its various derivatives are used in industries such as perfumery, pharmaceuticals and food manufacturing. Furthermore, this compound plays a pivotal role in the synthesis of allyl diglycol carbonate, poly(styrene-allyl alcohol), 1,3-propanediol and more, which serve as essential components in plasticizers, crosslinking agents and coating additives [1,2]. At present, allyl alcohol is primarily manufactured through the utilization of fossil fuels, as it is typically synthesized via the vapour-phase acetoxylation of petroleum-derived propylene, followed by hydrolysis in the liquid phase [3]. In light of the diminishing petroleum resources, the chemical industry is presently confronted with the task of creating bio-based production methods [4]. There are several renewable sources that can be considered potential starting materials for the production of allyl alcohol. Among these sources, glycerol stands out as the most promising option, particularly in regard to carbon efficiency. Glycerol is a by-product generated during the transesterification process of vegetable oils used in biodiesel production. To strengthen the sustainability of the biodiesel industry, not only a shift from edible to waste vegetable oil is required, but also the valorization of glycerol in large-scale processes [5]. Recently, Lari et al. studied the synthesis of allyl alcohol from glycerol via dehydration + hydrogenation reactions using a 5%Ag/ZSM-5 catalyst. This system yielded 21% of allyl alcohol under molecular hydrogen at 40 bar. They modelled the process by combining a gas-phase fixed-bed reactor, three flash separators, five distillation columns and a liquid–liquid extraction column. Nonetheless, the process is burdened by low selectivity, significant energy consumption due to the intricate separation steps, and the necessity to handle substantial volumes of wastewater, resulting in a notably high overall cost [5,6]. Overall, the necessity of a more selective process for allyl alcohol production, operating in continuous flow is evident.

As a substitute, the deoxydehydration (DODH) of glycerol to produce allyl alcohol was suggested, but this approach has received limited research attention. Generally, a DODH

reaction eliminates two neighbouring hydroxyl groups in vicinal diols, leading to the formation of the corresponding alkene, such as allyl alcohol when applied to glycerol [7,8]. In this reaction, a catalyst primarily based on rhenium is commonly employed, along with the need for a stoichiometric reductant, which can be either hydrogen ( $H_2$ ) or a secondary alcohol [9]. However, only a few systems of glycerol conversion to allyl alcohol with a cheap reductant have been reported on the scale [1,7]. We have recently reported the use of a heterogeneous Re-based catalyst (10%  $ReO_x/CeO_2$ ) for the efficient conversion of glycerol to allyl alcohol with 2-hexanol as a reductant and solvent [10]. The catalyst was highly stable, allowing its reuse for three cycles of reaction without any loss in activity. Correspondingly, these results are the starting point for the process simulation of the DODH reaction from glycerol to allyl alcohol using 2-hexanol as solvent and H-donor. In the current work, we aim to design a process for allyl alcohol production from glycerol over a Ceria-supported Rhenium oxide catalyst and evaluate the technical feasibility of the process. In the first step, the DODH reaction of glycerol to allyl alcohol was performed to obtain the kinetic data required for the design of the conversion operation. Furthermore, in order to improve the reliability of the separation process, accurate binary coefficients of UNIQUAC thermodynamic model were calculated using data regression of vapour–liquid equilibrium (VLE) reported in a previous study [11]. The kinetic data from the DODH reaction and the thermodynamic data from the VLE data regression were used for the simulation process performed using the Aspen Plus software. The simulated process consists of four processing subsystems: allyl alcohol synthesis via DODH reaction, solvent recovery, allyl alcohol purification through extractive distillation and solvent regeneration via catalytic hydrogenation.

## 2. Methodology

### 2.1. Catalyst Synthesis

The catalyst was prepared through the incipient wetness impregnation method according to [10]. Briefly, 2 g of Ceria support (HSA-5 commercialized by SOLVAY) was dried for 12 h at 110 °C before calcination at 500 °C in air. After the addition of 400 mg of  $HReO_4$  (75 wt.% commercialized by MERCK) in 0.75 mL water, the slurry was stirred for 2 h, before being dried at 110 °C for 12 h followed by a calcination at 500 °C (heating rate of 5 °C/min, 3 h) in static air. A detailed characterization of the catalyst was reported in reference [10].

### 2.2. DODH Reaction of Glycerol to Allyl Alcohol in Batch Conditions

The DODH of glycerol was performed in a PARR reactor of 50 mL nominal volume (Parr 4597) equipped with a mechanic stirrer. The latter was initially charged with 0.7 g of catalyst and 17 mL of 2-hexanol under an air atmosphere. Before beginning the reaction, the autoclave was flushed three times with nitrogen before being heated under stirring to the desired reaction temperature with a heating rate of 3 °C/min. When the final reaction temperature was reached, 8 mL of a solution containing 0.7 g of glycerol in 2-hexanol was introduced to the reactor by means of a pump with a flow rate of 10 mL/min. After 2 min, the reaction mixture was considered to be homogenized and the first sample (200  $\mu$ L) was taken, followed by periodic sampling every 15 min for the first 2 h (8 samples) of the reaction and every 30 min in the following 2 h (4 samples). The catalytic performance was calculated based on the glycerol concentration determined via gas chromatography with a column CP-Wax52CB (30 m  $\times$  250  $\mu$ m  $\times$  0.25  $\mu$ m) and a flame ionization detector (FID).

### 2.3. Hydrogenation of 2-Hexanone in Batch Conditions

The solvent regeneration that consists of the hydrogenation of 2-hexanone to 2-hexanol was performed in a Screening Pressure Reactor (SPR, Freeslate, Great Britain) consisting of 24 batch reactors (6 mL volume each), which operated all under the same pressure and temperature. The reaction was performed using two commercial catalysts, namely 5% Pd/C (Alfa Aesar, Schiltigheim, France) and 1 wt.% Pt/ $\gamma$ - $Al_2O_3$  (Alfa Aesar). Prior to

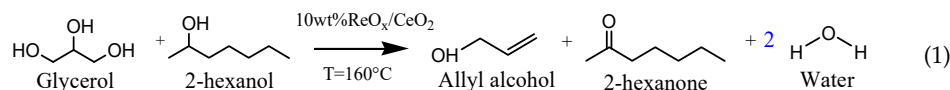
the catalytic test, both catalysts were reduced to a metallic state and stored under an inert atmosphere in order to avoid their re-oxidation when in contact with air. The reduction was performed for 3 h at 350 °C (temperature ramp of 5 °C/min) under pure hydrogen (30 mL/min) at 2.68 bar of pressure. Once the reduction protocol was completed, the catalyst was transferred to the reactor vessel in a glove box and charged with 2 mL of a solution containing 3 wt.% of 2-hexanone in 2-hexanol. The reaction was then performed under 4 bar of pure hydrogen atmosphere at a reaction temperature of 70 °C and a stirring speed of 600 rpm for 6 h. The catalytic performance was determined by measuring the 2-hexanone concentration using the same gas chromatograph equipment as described in Section 2.2 for the DOHD reaction of glycerol.

#### 2.4. Modelling and Simulation of the Whole Process

The simulation process of the allyl alcohol synthesis from glycerol with 2-hexanol as a solvent and H-donor was performed using Aspen Plus software (Aspen technology Inc., New Bedford, MA, USA). The simulation was performed for a plant capacity of 550.000 m<sup>3</sup>/a of allyl alcohol, corresponding to a glycerol molar flowrate of 960 mol/h. The process consists of four processing subsystems: allyl alcohol synthesis (S1), solvent recovery (S2), allyl alcohol purification through extractive distillation (S3) and solvent regeneration through catalytic hydrogenation (S4), which will be detailed in Section 3.4.

##### 2.4.1. Allyl Alcohol Synthesis

A continuous stirred tank reactor (CSTR) module is used to simulate the DODH reaction of glycerol to allyl alcohol at a steady state. Equation (1) shows the reaction used for reactor modelling with 2-hexanol. The reaction kinetic model was assumed to follow the power law model based on experimental data obtained in batch conditions. The pressure of the reaction was adjusted according to the conversion rate value at a steady state, which was acquired from experimental data in continuous flow conditions.



##### 2.4.2. Solvent Recovery

Since the deoxydehydration of glycerol yields allyl alcohol in low concentration (0.03 mole fraction in 2-hexanol), the recovery of allyl alcohol and 2-hexanol is highly important. In addition, according to the DODH reaction (Equation (1)), water and 2-hexanone are formed as by-products. In fact, the solvent acts hereby as a hydrogen donor and becomes oxidized to the corresponding ketone. Therefore, to improve the reliability of the column distillation unit, binary coefficients based on the UNIQUAC thermodynamic model were employed (Equation (2)). The binary coefficients of mixtures such as allyl/2-hexanone, allyl/2-hexanol and 2-hexanone/2-hexanol obtained via data regression of vapour–liquid equilibrium (VLE), were taken from [11]. Allyl alcohol/water, 2-hexanol/water and 2-hexanone/water binary coefficients were obtained from the Aspen Plus database. Concerning binary mixtures with glycerol, vapour–liquid equilibria (VLE) were predicted by the UNIFAC-DMD thermodynamic model. The binary coefficients are presented in Table 1, entries 4–6.

The resulting reaction mixture from the DODH reactor was separated on a distillation column to recover all product on the top and most of the solvent on the bottom. The evaluation of the distillation processes was conducted by employing both simplified shortcut methods and rigorous models that are accessible within the simulation software package. The short-cut method DSTWU included in Aspen Plus is based on the equation and correlation of Winn–Underwood–Gilliland that allows obtaining preliminary specifications such as the minimum number of theoretic stages, the minimum reflux ratio, the distillate-to-feed ratio, the location of the feed stage and the product split—for a mole recovery of the most light-weight and heavy-weight components, in the distillate stream. With this information, the rigorous model was performed using a RADFRAC column, based on the equilibrium

method, which is based on the MESH equations (mass, equilibrium, summation and heat equations) and using the inside-out algorithm [12]. This column is used mainly for all multistage vapour–liquid fractionation operations. Finally, a series of sensitivity analyses were carried out to investigate how the primary operational variables, including reflux ratio, number of stages and distillate-to-feed ratio, impact both the purity and recovery of allyl alcohol.

**Table 1.** Parameters of the binary mixture employed in the UNIQUAC model.

Entry	Component i	Component j	A <sub>ij</sub>	A <sub>ji</sub>	B <sub>ij</sub>	B <sub>ji</sub>	Ref.
1	Allyl Alcohol	2-Hexanol	0.205708	−0.266409	−205.474	178.806	[11]
2	Allyl Alcohol	2-Hexanone	−0.554112	1.49424	296.834	−737.781	[11]
3	2-Hexanone	2-Hexanol	−2.63732	4.67125	1208.08	−2074	[11]
4	Allyl Alcohol	Water	2.8583	−2.9539	−1078.13	925.896	APV90 VLE-IG
5	2-Hexanol	Water	0	0	−552.14	73.5103	APV90 VLE-IG
6	2-Hexanone	Water	1.6266	1.6266	1.6266	1.6266	APV90 LLE-ASPEN
7	Allyl Alcohol	N-Methyl-2-pyrrolidone	−4.0312	1.1989	1265.26	−280.81	[13]
8	Allyl Alcohol	Glycerol	−0.400453	1.1989	−0.400453	−0.400453	UNIFAC-DMD
9	2-Hexanol	Glycerol	−0.562681	0.270421	18.2592	−110.508	UNIFAC-DMD
10	2-Hexanone	Glycerol	−0.445955	0.248209	−351.388	−25.5053	UNIFAC-DMD
11	2-Hexanol	N-Methyl-2-pyrrolidone	1.54778	−3.1722	−373.4	983.268	UNIFAC-DMD
12	2-Hexanone	N-Methyl-2-pyrrolidone	0.265205	−0.280694	66.428	−118.297	UNIFAC-DMD
13	Glycerol	N-Methyl-2-pyrrolidone	12.0093	−21.0165	−6253.61	11070.1	UNIFAC-DMD

Equation of UNIQUAC thermodynamic model:

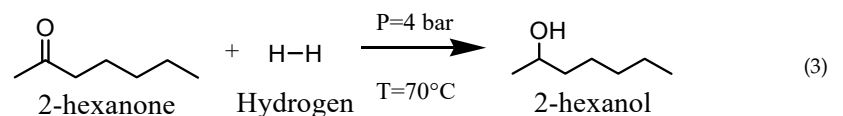
$$\begin{aligned}
 \ln \gamma_i &= \ln \frac{\phi_i}{x_i} + \frac{z}{2} q_i \ln \frac{\theta_i}{\phi_i} - q_i' \ln t_i' - q_i' \sum_j \frac{\theta_j' \tau_{ij}}{t_j} + l_i + q_i' - \frac{\phi_i}{x_i} \sum_j x_j l_j \\
 \theta_i &= \frac{q_i x_i}{q_T} ; q_T = \sum_k q_k x_k & \theta_j' &= \frac{q_j' x_j}{q_T'} ; q_T' = \sum_k q_k' x_k \\
 \phi_i &= \frac{r_i x_i}{r_T} ; r_T = \sum_k r_k x_k & l_j &= \frac{z}{2} (r_i - q_i) + 1 - r_i \\
 t_i' &= \sum_k \theta_k' \tau_{ki} & \tau_{ij} &= \exp \left( A_{ij} + \frac{B_{ij}}{T} \right) \\
 & & z &= 10
 \end{aligned} \tag{2}$$

#### 2.4.3. Allyl Alcohol Purification

The resulting distillate was sent to an extractive distillation column to perform the product purification. The column simulation was based on the Aspen plus Radfrac routine. The design variables were the purity of allyl alcohol in the distillate and bottom stream of 0.965 and 0.001 (mole fraction), adjusted by the distillate flowrate and reflux ratio, respectively. Later, the RADFRAC column simulation was performed, followed by sensitivity analyses.

#### 2.4.4. Solvent Regeneration

In order to obtain an eco-friendly and economical process, 2-hexanol should be regenerated from 2-hexanone. In this light, the solvent-rich bottom stream coming from the distillation column was directed to a hydrogenation reactor in order to perform the solvent regeneration, before subsequent recycling to the DODH reactor. Since the kinetic data of the reaction is unknown, a Stoichiometric reactor (RStoic) module was used. Equation (3) shows the reaction used for reactor modelling.



### 3. Results and Discussion

#### 3.1. Kinetic Parameters of DODH Reaction

The concentration vs. time profile for the DODH reaction using the Ceria-supported Rhenium catalyst (10%ReO<sub>x</sub>/CeO<sub>2</sub>) in 2-hexanol at temperatures of 140 °C and 150 °C, is dis-

played in Figure 1. Based on the excess of 2-hexanol, the reaction rate of glycerol was assumed to follow a first-order reaction. Correspondingly, the curves were fitted to obtain the first-order rate constant ( $k_i$ ). The observed kinetic constants were  $8.32 \times 10^{-5} \text{ s}^{-1}$  and  $1.22 \times 10^{-4} \text{ s}^{-1}$  at  $140^\circ\text{C}$  and  $150^\circ\text{C}$ , respectively. Correspondingly, the activation energy in this reaction was estimated to be  $54.9 \text{ kJ/mol}$ . The activation energy in this reaction system is only slightly higher than that observed for the homogeneous DODH of glycerol ( $25.1 \text{ kJ/mol}$ ) [13], but lower than for the DODH reaction of glycerol using a heterogeneous catalyst based on rhenium oxide nanoparticles ( $\text{ReO}_x$  NPs,  $97 \text{ kJ/mol}$ ) [14]. Thermodynamic parameters were determined from observed kinetic constants at corresponding temperatures. Data fitting of the Eyring equation gave an enthalpy of  $\Delta H = 52.32 \text{ kJ mol}^{-1}$  and entropy of  $\Delta S = -199.0 \text{ J mol}^{-1} \text{ K}^{-1}$  at  $150^\circ\text{C}$ .

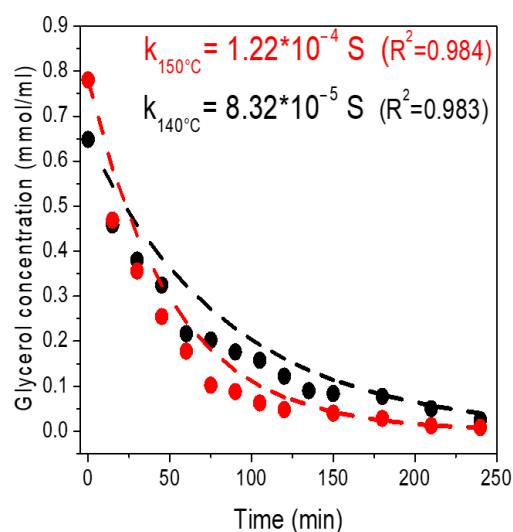


**Figure 1.** Concentration vs. time profile for the glycerol DODH to allyl alcohol at  $140^\circ\text{C}$  and  $150^\circ\text{C}$ . Conditions: 700 mg of catalyst ( $10\% \text{ReO}_x/\text{CeO}_2$ ), 700 mg glycerol in 2-hexanol, 25 mL of volume.

### 3.2. Hydrogenation of 2-Hexanone

The hydrogenation of 2-hexanone was studied over two commercial catalysts, namely 5% Pd/C (Alfa Aesar) and 1 wt.% Pt/ $\gamma\text{-Al}_2\text{O}_3$  (Alfa Aesar). As one can see from Figure 2, both catalysts exhibit a selectivity of  $>99\%$  to 2-hexanol. On the other hand, 5% Pd/C (Alfa Aesar) was only poorly active with a low conversion of no more than 8%, whereas the catalyst based on 1 wt.% Pt/ $\gamma\text{-Al}_2\text{O}_3$  achieved full conversion of 2-hexanone. The latter finding agrees with prior literature, which has demonstrated that platinum exhibits exceptional catalytic efficacy in the hydrogenation of ketones under mild operating conditions [15,16].

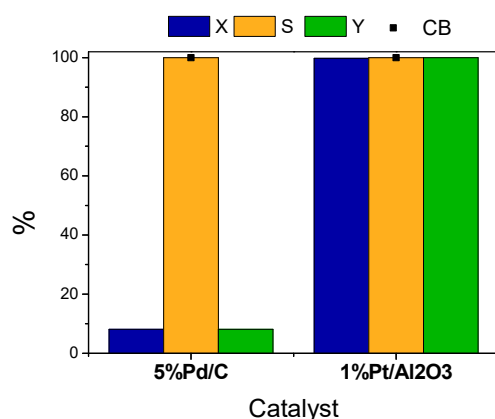


**Figure 2.** Catalytic performance of hydrogenation of 2-hexanone into 2-hexanol,  $T = 70^\circ\text{C}$ ,  $P_{\text{H}_2} = 4 \text{ bar}$ , stirring speed = 600 rpm, 2 hexanone concentration = 3 wt.%.

### 3.3. Modelling Process

The process for a large-scale synthesis of allyl alcohol from glycerol was modelled based on the aforementioned experimental results (Sections 3.1 and 3.2) using Aspen Plus. The process flow diagram is shown in Figure 3. The process consists of four subsystems:

- Allyl alcohol production (S1): Five continuously stirred tank reactors for the DODH reaction of glycerol to allyl alcohol in the presence of 2-hexanol. These reactors will be designed to achieve a maximum conversion of glycerol.
- Solvent recovery (S2): A distillation column for the separation of Allyl alcohol from the reaction mixture. This column will be designed to guarantee the recovery of the entire allyl alcohol from the DODH at the top.
- Allyl alcohol purification (S3): Purification of allyl alcohol using N-Methyl-2-pyrrolidone as an entrainer. This section will be designed to achieve the highest purity of allyl alcohol at the minimum loss of entrainer and product.
- Solvent regeneration (S4): Hydrogenation of 2-hexanone formed in the DODH reaction to obtain 2-hexanol.

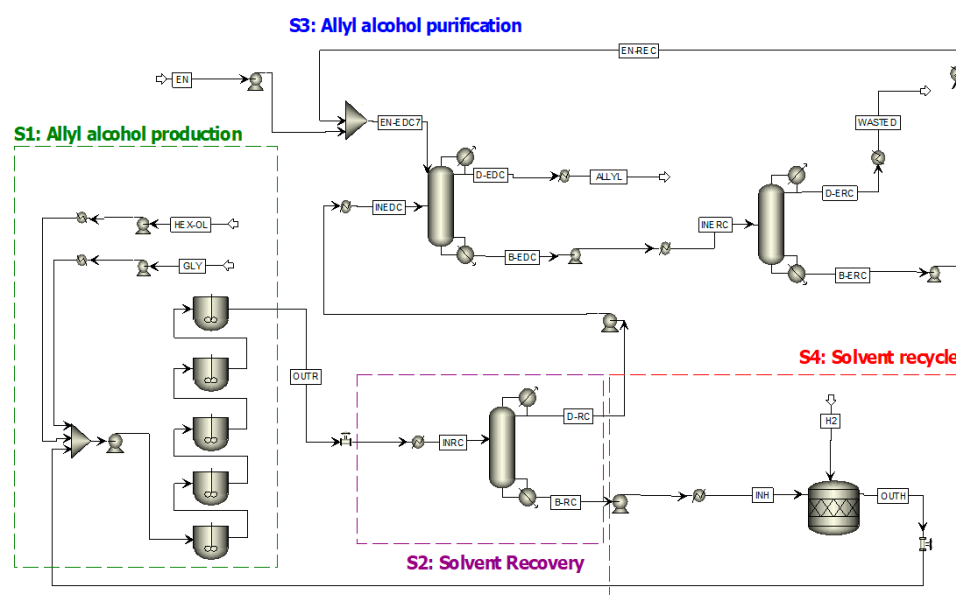


**Figure 3.** Integrated process flow diagram for the synthesis of allyl alcohol via DODH reaction, including product purification through extractive distillation and solvent regeneration through hydrogenation.

#### 3.3.1. Allyl Alcohol Production (S1)

The deoxydehydration (DODH) of glycerol was modelled employing a cascade of five identical CSTR reactors at 170 °C aiming for 96% yield in allyl alcohol (96% conversion, 100% selectivity). The kinetic constants were extrapolated to a reaction temperature of 170 °C based on the results previously presented in Section 3.1, with a glycerol/ReO<sub>x</sub> mass ratio of 10. The total resident time ( $\tau$ ) was calculated to be 24.3 min, resulting in a total volume for the reaction of 1.54 m<sup>3</sup> with a fixed flow rate of 3.8 m<sup>3</sup>/h. The corresponding parameters of the model are given in Table 2.

**Table 2.** DODH reactor—modelling parameters.

Conversion ( $X_{GLY}$ ) [%]	96
$k$ (170 °C) [ $s^{-1}$ ]	$3.09 \times 10^{-3}$
Volume [m <sup>3</sup> ]	1.54
$\tau$ (total) [min]	24.3

### 3.3.2. Solvent Recovery (S2)

The resulting rich 2-hexanol mixture containing allyl alcohol was sent to the solvent recovery subsystem (S2), containing a RADFRAC distillation column. Sensitivity analysis results are shown in Figure 4. As observed, a recovery of 99.99% of allyl alcohol in the distillate ( $R_{\text{Allyl}}^D$ ) could be obtained for different combinations of the number of stages (NS) and reflux ratio (RR). However, an increase in the reflux ratio directly resulted in a higher recovery of 2-hexanol in the bottom stream. Thus, the optimal reflux ratio was  $1.5R_{\text{min}}$  with corresponding  $2.14N_{\text{min}}$ . The optimal parameters of the distillation are given in Table 3.

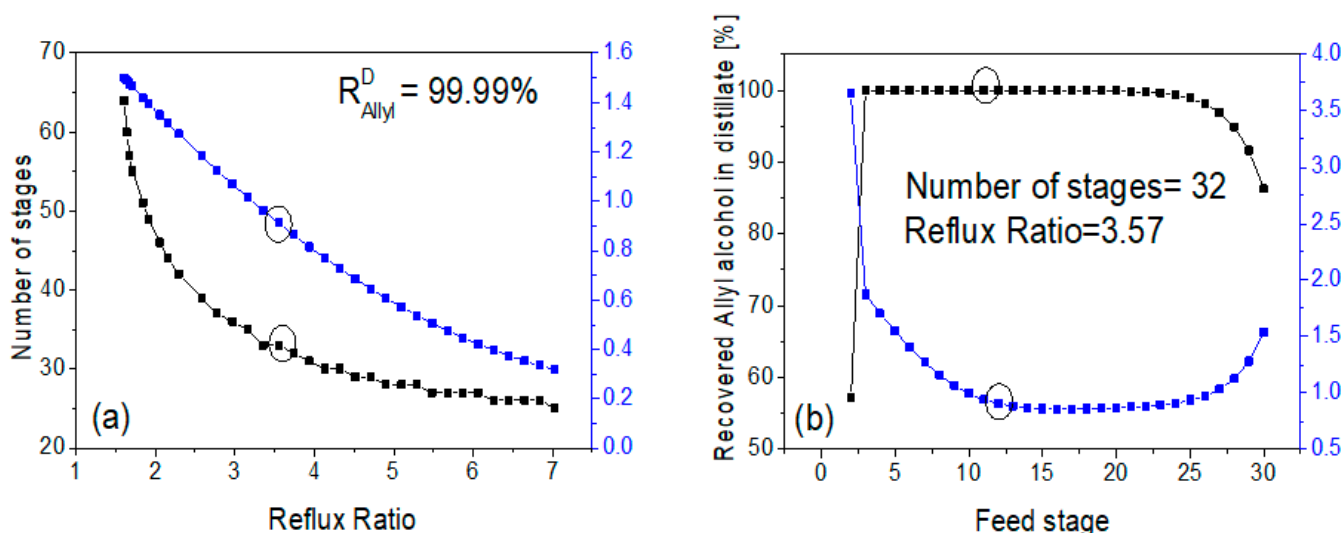


**Figure 4.** Effect of the reflux ratio (a) and the number of stages (b) on the allyl alcohol recovery and 2-hexanol loss [17]. The circled stage and reflux ratio correspond to the optimal parameters.

**Table 3.** Optimal operation conditions for the recovery column (RC) [17].

Optimum number of stages (NS)	32
Minimum number of stages ( $N_{\text{min}}$ )	14.8
Optimum reflux ratio (RR)	3.57
Minimum reflux ratio ( $R_{\text{min}}$ )	2.38
Distillate-to-feed ratio (DTFR)	0.126
Feed stage (FS)	12
Feed temperature [ $^{\circ}\text{C}$ ]	124.8
Reboiler temperature [ $^{\circ}\text{C}$ ]	145.3
Condenser temperature [ $^{\circ}\text{C}$ ]	88.7

### 3.3.3. Purification of Allyl Alcohol (S3)

The designs of the two distillation columns for the purification of allyl alcohol (extractive distillation column—EDC; entrainer recovery column—ERC) were performed, including a sensitivity analysis aiming for purity in allyl alcohol of 99.99%. From Figure 5a, one can see that the minimum number of stages ( $N_m$ ) was 23 for an entrainer-to-feed ratio (ENTFR) of 19. For the optimisation, the number of stages was fixed to twice  $N_m$ , meaning 46 stages. With this fixed number of stages, the influence of the reflux ratio (RR) on the entrainer-to-feed ratio (ENTFR) was studied (Figure 5b). The range of the reflux ratio was, therefore, varied between 1 and 4 to minimize the entrainer-to-feed ratio. From the results (Figure 5b), one can see that a plateau is reached for a reflux ratio between 2.72 and 3.5. Of course, the lowest value (2.72) is the most favourable and was thereby used for the optimisation of the distillate-to-feed ratio for a fixed reflux ratio of 2.72 and 46 stages. As

seen in Figure 5c, it is possible to recover nearly the entire amount of allyl alcohol with very high purity using a distillate-to-feed ratio (DTFR) of 0.2775. However, when increasing the allyl alcohol recovers from 99.8 to 99.9%, the amount of required entrainer sharply increases. The optimized design parameters are given in Table 4.

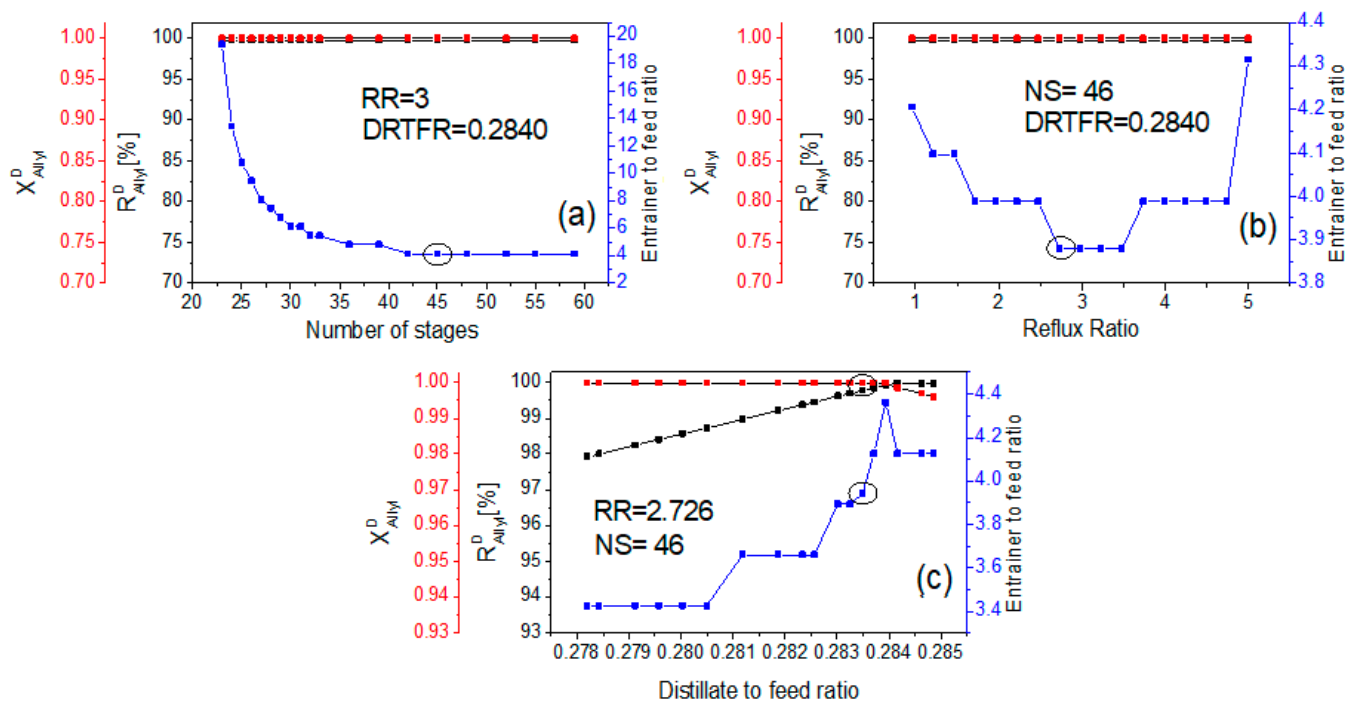


**Figure 5.** Sensitivity analysis of the extractive distillation column (EDC) for the optimum number of stages (a), the optimum reflux ratio (b) and the optimum distillate to feed ratio (c).  $x_{Alyl}^D$  [%] = allyl alcohol mole fraction in the distillate,  $R_{Alyl}^D$  [%] = recovered allyl alcohol in the distillate [17]. The circled stage, reflux ratio and distillate to feed ratio correspond to the optimal parameters.

**Table 4.** Optimal operation conditions for the extractive distillation column (EDC) [17].

Optimum number of stages (NS)	46
Minimum number of stages ( $N_m$ )	23
Optimum reflux ratio (RR)	2.72
Distillate-to-feed ratio (DRTFR)	0.284
Feed stage (FS)	18
Entrainer-to-feed ratio (ENTFR)	3.87
Entrainer feed stage (FS)	5
Feed inlet temperature [°C]	106.32
Entrainer feed inlet temperature [°C]	83
Reboiler temperature [°C]	184.36
Condenser temperature [°C]	96.76

### 3.3.4. Solvent Regeneration (S4)

The solvent regeneration through hydrogenation of the 2-hexanone was simulated using a Stoichiometric reactor (RStoic), fixing the yield to 99.85%. This conversion was deliberately chosen according to the results from the hydrogenation reaction, previously discussed (cf. Section 3.2), using the 1 wt.% Pt/ $\gamma$ - $Al_2O_3$  catalyst at 4 bar and 70 °C.



### 3.4. Energy and Mass Balance

Finally, the total mass balance is given in Table 5. The results showed that the whole process had 96% overall glycerol-to-allyl molar yield, producing 53.519 kg/h of highly pure allyl alcohol (99.99 wt%) from 88.406 kg/h of glycerol. The loss of allyl alcohol was limited to less than 0.2% (0.123 kg/g). The loss of entrainer (N-Methyl-2-pyrrolidone) was also very low with no more than 0.01 Kg/h of entrainer required to be replaced. On the other hand, the results also showed that the main drawback of the process lies in the significant loss of the solvent (2-hexanol) and the corresponding ketone (2-hexanone). In fact, for 1 mol/h allyl alcohol produced, 0.5 mol/h of solvent must be introduced to the process in order to compensate for the loss of 2-hexanol (0.209 mol/h) and 2-hexanone (0.291 mol/h). This was also visible when calculating the overall process yield (OPY, Equation (4)), which corresponds to the ratio of moles of product stream (allyl alcohol) to moles of input streams (glycerol, 2-hexanol, hydrogen, entrainer). The latter reached only 45% in the present case, due to the large loss of 2-hexanol.

$$OPY = \frac{n_{Allyl}}{n_{Gly} + n_{Hex-ol} + n_{H_2} + n_{En}} * 100\% \quad (4)$$

**Table 5.** Mass balance of the process [17].

Inlet streams	Glycerol [Kg/h]	88.406 (0.960) <sup>a</sup>
	2-hexanol [Kg/h]	51.097 (0.5)
	Entrainer [Kg/h]	0.01 (1 × 10 <sup>-4</sup> )
	Hydrogen [Kg/h]	1.349 (0.669)
	<b>Total inlet flow [Kg/h]</b>	<b>140.862 (2.129)</b>
Outlet streams	Allyl alcohol [Kg/h]	53.519 (0.922)
	Allyl alcohol purity [wt.%]	0.9999
	Total waste [Kg/h]	87.343 (3.379)
	Loss in Allyl alcohol [Kg/h]	0.123 (2.12 × 10 <sup>-3</sup> )
	2-hexanol loss [Kg/h]	21.312 (0.209)
	2-hexanone loss [Kg/h]	29.109 (0.291)
	<b>Total outlet flow [Kg/h]</b>	<b>140.826 (3.379)</b>
Overall process yield OPY [%]		45.0

<sup>a</sup> molar flow rate in [kmol/h] in brackets.

Next to the mass balance, the energy input and output were determined using an ASPEN energy analyser. The energy consumption was thereby estimated using the heat required by the reboilers, heat exchangers, reactors and condensers, as well as the electricity for the pumps and reactors. The total energy required by the process utilities was therefore 1.344 MW, corresponding to steam, electricity and cooling water (Table 6). Since the main consumption was from the cooling water (680.8 kW), optimisation was performed by designing an integrated heat exchange network. The latter allowed to reduce the required energy of the process by 35.8%, corresponding to a gain of 481 kW. The energy balance further allowed for the calculation of the carbon footprint of the process, which can be expressed in mass of CO<sub>2</sub> equivalents per hour—corresponding to 100.8 kgCO<sub>2</sub>/h—or mass of CO<sub>2</sub> equivalents per mass of product—corresponding to 1.89 kgCO<sub>2</sub>/kgAllylOH. Even though these values do not correspond to greenhouse gas emissions as they are calculated in a rigorous life cycle assessment, it allows us to roughly compare this process to the fossil-based process. In the literature, no study was found for the classical production process of allyl alcohol from propylene. However, since allyl alcohol is currently obtained through a two-step process with acrolein as an intermediate, we decided to compare our DODH process to the production of acrolein from glycerol via catalytic dehydration. The latter was reported to emit 3.0 kgCO<sub>2</sub>/kgAcrolein, which is 50% more than our process [18]. The

present process can thus be considered eco-friendlier than an alternative production of allyl alcohol via dehydration of glycerol and followed hydrogenation of acrolein. Furthermore, the energy efficiency was calculated according to Equation (5). The latter is defined as the ratio between the energy contained in the outflow and the sum of the inflow and net primary energy and corresponds to 20.8%.

$$\text{Energy Eff.} = \frac{\text{Output flow energy}}{\text{Input flow energy} + \text{net primary energy}} * 100\% \quad (5)$$

**Table 6.** Energy balance of the process [17].

High-pressure steam [kW]	177.2
Medium-pressure steam [kW]	214.9
Low-pressure steam [kW]	42.5
Electricity [kW]	229.1
Cooling water [kW]	680.8
Total energy in utilities [kW]	1344.6
Energy savings [kW] <sup>a</sup>	481.1
Net primary energy (NPE) [kW] <sup>b</sup>	863.5
Input flow energy [kW]	231.6
Output flow energy [kW]	248.7
Energy efficiency [%]	20.8
Carbon footprint [kgCO <sub>2</sub> /h]	100.8

<sup>a</sup> Obtained with ASPEN Energy Analyzer. <sup>b</sup> NPE = total energy in utilities—energy savings.

#### 4. Conclusions

A process for the synthesis of allyl alcohol was modelled based on the DODH reaction of glycerol. The reaction took place using 10%ReO<sub>x</sub>/CeO<sub>2</sub> as a catalyst, with 2-hexanol as H-donor and solvent. The process was designed for a glycerol flow rate of 1 kmol/h, corresponding to a plant capacity of 550.000 m<sup>3</sup>/a of allyl alcohol. In order to have a high accuracy of the model, the rate constant of the DODH reaction was determined experimentally, supposing pseudo-homogeneous kinetics. The reaction was implemented in a cascade of five CSTRs in order to achieve an allyl alcohol yield of 96%. After solvent separation and recycling, the purification of allyl alcohol yielded a purity of 99.99%, with only very little loss of product (0.2%). The main drawback identified was the significant loss of 2-hexanol, which corresponded nearly to 0.5 moles per mole of produced allyl alcohol. From the energetic point of view, the process integration was optimized, reducing the net primary energy input to 863.5 kW, which corresponded to a carbon footprint of 1.89 kgCO<sub>2</sub>/kgAllylOH. This process simulation provides a first indication of the viability of allyl alcohol synthesis from glycerol at a large scale.

**Author Contributions:** Conceptualization, B.K. and M.A.; methodology, M.A.; investigation, K.S.V. and G.A.; data curation, K.S.V. and G.A.; writing—original draft preparation, K.S.V.; writing—review and editing, B.K. and G.A.; supervision, B.K. and M.A.; project administration, B.K. and M.A. All authors have read and agreed to the published version of the manuscript.

**Funding:** This research received no external funding.

**Data Availability Statement:** All data are contained within the article.

**Conflicts of Interest:** The authors declare no conflict of interest.

#### References

1. Tazawa, S.; Ota, N.; Tamura, M.; Nakagawa, Y.; Okumura, K.; Tomishige, K. Deoxydehydration with Molecular Hydrogen over Ceria-Supported Rhenium Catalyst with Gold Promoter. *ACS Catal.* **2016**, *6*, 6393–6397. [CrossRef]
2. Sánchez, G.; Dlugogorski, B.Z.; Kennedy, E.M.; Stockenhuber, M. Zeolite-supported iron catalysts for allyl alcohol synthesis from glycerol. *Appl. Catal. A Gen.* **2016**, *509*, 130–142. [CrossRef]

3. Meiko, S.; Hiroshi, U. Production Process of Allyl Alcohol, and Allyl Alcohol Obtained by the Production Processes. U.S. Patent Application 2006/0084829 A1, 20 April 2006.
4. Buitelaar, M.M.; Van Daatselaar, E.; Van Teijlingen, D.G.; Stokvis, H.I.; Wendt, J.D.; De Sousa Ribeiro, R.J.; Brooks, A.M.M.; Kamphuis, E.C.; Lopez Montoya, S.; Van Putten, J.C.; et al. Process Designs for Converting Propylene Glycol to Acrylic Acid via Lactic Acid and Allyl Alcohol. *Ind. Eng. Chem. Res.* **2020**, *59*, 1183–1192. [[CrossRef](#)]
5. Lari, G.M.; Pastore, G.; Haus, M.; Ding, Y.; Papadokonstantakis, S.; Mondelli, C.; Pérez-Ramírez, J. Environmental and economical perspectives of a glycerol biorefinery. *Energy Environ. Sci.* **2018**, *11*, 1012–1029. [[CrossRef](#)]
6. D'Angelo, S.C.; Dall'Ara, A.; Mondelli, C.; Pérez-Ramírez, J.; Papadokonstantakis, S. Techno-Economic Analysis of a Glycerol Biorefinery. *ACS Sustain. Chem. Eng.* **2018**, *6*, 16563–16572. [[CrossRef](#)]
7. Canale, V.; Tonucci, L.; Bressan, M.; D'Alessandro, N. Deoxydehydration of glycerol to allyl alcohol catalyzed by rhenium derivatives. *Catal. Sci. Technol.* **2014**, *4*, 3697–3704. [[CrossRef](#)]
8. Tshibalonza, N.N.; Monbaliu, J.C.M. Revisiting the deoxydehydration of glycerol towards allyl alcohol under continuous-flow conditions. *Green Chem.* **2017**, *19*, 3006–3013. [[CrossRef](#)]
9. Boucher-Jacobs, C.; Nicholas, K.M. Catalytic deoxydehydration of glycols with alcohol reductants. *ChemSusChem* **2013**, *6*, 597–599. [[CrossRef](#)] [[PubMed](#)]
10. Silva Vargas, K.; Zaffran, J.; Araque, M.; Sadakane, M.; Katryniok, B. Deoxydehydration of glycerol to allyl alcohol catalysed by ceria-supported rhenium oxide. *Mol. Catal.* **2023**, *535*, 112856. [[CrossRef](#)]
11. Silva Varga, K.; Katryniok, B.; Araque, M. Isobaric Vapor–Liquid Equilibrium Data for Six Binary Systems: Prop-2-en-1-ol (1)–Hexan-2-ol (2), Prop-2-en-1-ol (1)–Hexan-2-one (2), Hexan-2-one (1)–Hexan-2-ol (2), Prop-2-en-1-ol (1)–4-Methyl-pentan-2-ol (2), Prop-2-en-1-ol (1)–4-Methyl-pentan-2-one (2), and 4-Methyl-pentan-2-one (1)–4-Methyl-pentan-2-ol (2) at 101.32 kPa. *J. Chem. Eng. Data* **2021**, *66*, 1055–1067.
12. Quintero, J.A.; Cardona, C.A. Process simulation of fuel ethanol production from lignocellulosics using aspen plus. *Ind. Eng. Chem. Res.* **2011**, *50*, 6205–6212. [[CrossRef](#)]
13. Qu, S.; Dang, Y.; Wen, M.; Wang, Z.X. Mechanism of the methyltrioxorhenium-catalyzed deoxydehydration of polyols: A new pathway revealed. *Chem. Eur. J.* **2013**, *19*, 3827–3832. [[CrossRef](#)] [[PubMed](#)]
14. Jang, J.H.; Sohn, H.; Camacho-Bunquin, J.; Yang, D.; Park, C.Y.; Delferro, M.; Abu-Omar, M.M. Deoxydehydration of Biomass-Derived Polyols with a Reusable Unsupported Rhenium Nanoparticles Catalyst. *ACS Sustain. Chem. Eng.* **2019**, *7*, 11438–11447. [[CrossRef](#)]
15. McManus, I.; Daly, H.; Thompson, J.M.; Connor, E.; Hardacre, C.; Wilkinson, S.K.; Sedaie Bonab, N.; Ten Dam, J.; Simmons, M.J.H.; Stitt, E.H.; et al. Effect of solvent on the hydrogenation of 4-phenyl-2-butanone over Pt based catalysts. *J. Catal.* **2015**, *330*, 344–353. [[CrossRef](#)]
16. Alonso, F.; Riente, P.; Rodríguez-Reinoso, F.; Ruiz-Martínez, J.; Sepúlveda-Escribano, A.; Yus, M. A highly reusable carbon-supported platinum catalyst for the hydrogen-transfer reduction of ketones. *ChemCatChem* **2009**, *1*, 75–77. [[CrossRef](#)]
17. Silva, K. Upscaling Allyl Alcohol Synthesis from Glycerol. Ph.D. Thesis, Université de Lille, Lille, France, 2020.
18. Cespi, D.; Passarini, F.; Mastragostino, G.; Vassura, I.; Larocca, S.; Iaconi, A.; Chiericato, A.; Dubois, J.-L.; Cavani, F. Glycerol as feedstock in the synthesis of chemicals, a life cycle analysis for acrolein production. *Green Chem.* **2015**, *17*, 343–355. [[CrossRef](#)]

**Disclaimer/Publisher's Note:** The statements, opinions and data contained in all publications are solely those of the individual author(s) and contributor(s) and not of MDPI and/or the editor(s). MDPI and/or the editor(s) disclaim responsibility for any injury to people or property resulting from any ideas, methods, instructions or products referred to in the content.